Geoscience Frontiers xxx (2016) 1–14

HOSTED BY

ELSEVIER

Contents lists available at ScienceDirect

China University of Geosciences (Beijing)

Geoscience Frontiers

journal homepage: www.elsevier.com/locate/gsf

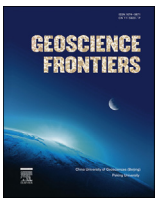

Research paper

Future changes in rainfall, temperature and reference evapotranspiration in the central India by Least Square Support Vector Machine

Sananda Kundu*, Deepak Khare, Arun Mondal

Department of Water Resources Development and Management, Indian Institute of Technology, Roorkee, India

ARTICLE INFO

Article history:
Received 17 February 2016
Received in revised form
20 May 2016
Accepted 2 June 2016
Available online xxx

Keywords:
Rainfall
Temperature
Reference evapotranspiration (ET_0)
Downscaling
Least Square Support Vector Machine (LS-SVM)

ABSTRACT

Climate change affects the environment and natural resources immensely. Rainfall, temperature and evapotranspiration are major parameters of climate affecting changes in the environment. Evapotranspiration plays a key role in crop production and water balance of a region, one of the major parameters affected by climate change. The reference evapotranspiration or ET_0 is a calculated parameter used in this research. In the present study, changes in the future rainfall, minimum and maximum temperature, and ET_0 have been shown by downscaling the HadCM3 (Hadley Centre Coupled Model version 3) model data. The selected study area is located in a part of the Narmada river basin area in Madhya Pradesh in central India. The downscaled outputs of projected rainfall, ET_0 and temperatures have been shown for the 21st century with the HADCM3 data of A2 scenario by the Least Square Support Vector Machine (LS-SVM) model. The efficiency of the LS-SVM model was measured by different statistical methods. The selected predictors show considerable correlation with the rainfall and temperature and the application of this model has been done in a basin area which is an agriculture based region and is sensitive to the change of rainfall and temperature. Results showed an increase in the future rainfall, temperatures and ET_0. The temperature increase is projected in the high rise of minimum temperature in winter time and the highest increase in maximum temperature is projected in the pre-monsoon season or from March to May. Highest increase is projected in the 2080s in 2081–2091 and 2091–2099 in maximum temperature and 2091–2099 in minimum temperature in all the stations. Winter maximum temperature has been observed to have increased in the future. High rainfall is also observed with higher ET_0 in some decades. Two peaks of the increase are observed in ET_0 in the April–May and in the October. Variation in these parameters due to climate change might have an impact on the future water resource of the study area, which is mainly an agricultural based region, and will help in proper planning and management.

1. Introduction

With the increasing population and demand, the availability of water per capita is decreasing. Uneven distribution of water resources both spatially and temporally is further making the situation more complicated along with the added impact of climate changes. The world climate is continually changing with the increasing concentration of carbon dioxide and other trace gases (Kamga, 2001). It has deep implication in the water resource management and future planning. According to the Central Water Commission (2005), the water availability per capita has reduced from 5176 m^3 in 1951 to about 1588 m^3 in 2010 in India, which was predicted to decline further in 2025 up to 1434 m^3. Changes in the climatic parameters are altering the water balance of a region and emergency measures should be taken for planning and management of the existing water resources. It is also necessary to assess the future impact of climate change on the water balance of a region to ensure proper planning and optimum use of the present water resources. Several models have been developed to understand the complex process of the hydrologic system (Arnold and Allen, 1996). Among these, many models involve the watershed heterogeneity, spatial distribution of vegetation, soil properties, topography, evaporation, rainfall and landuse like ANSWERS (Areal

* Corresponding author.
E-mail address: sanandakundu@gmail.com (S. Kundu).
Peer-review under responsibility of China University of Geosciences (Beijing).

http://dx.doi.org/10.1016/j.gsf.2016.06.002

Non-Point Source Watershed Environment Response Simulation) (Beasley et al., 1977) and agricultural nonpoint source (AGNPS) (Young et al., 1987, 1989), Soil Water Assessment Tool (SWAT) (Arnold et al., 1993; Rouhani et al., 2007; Thampi et al., 2010; El-Sadek et al., 2011; Shi et al., 2013), European hydrological system (MIKE SHE) (Abbott et al., 1986) and Water Erosion Prediction Project (WEPP) (Laflen et al., 1991). Gosain et al., (2009) reported that among the various available models, the semi-distributed hydrological models are more useful. The impacts of climate change have affected the water balance, resulting in an increasing disparity between the demand and supply of water that has resulted in greater attention to the planning of water resources (Guo et al., 2002).

Different studies (Hulme et al., 2002; Fowler et al., 2005) indicated that climate change due to anthropogenic factors have resulted in temperature changes leading to corresponding changes in the rainfall variability and spatial distribution, which further causes changes in the characteristics of the future runoff. Therefore, careful planning is required for the management of water resources and future adaptation. Different climate models are predicting the continuous rise of highly intense rainfall events in the 21st century (IPCC, 2007). Climate change effects on the monsoon rainfall of Southeast Asia has also been reported by Loo et al. (2015). Changes in the global climate have alarmed everyone to know about the future climate and its effect. As the General Circulation Models (GCMs) cannot be utilized directly for any regional hydrological models (Wigley et al., 1990; Carter et al., 1994), statistical techniques of downscaling are serving the purpose because it can relate global climatic variables with the local meteorological or hydrological variables. Many studies have used statistical relations between the monthly or annual rainfall and the soil erosion by rainfall from the outputs of GCM at large scale (Yang et al., 2003; Zhang et al., 2005; Ito, 2007). Statistical downscaling utilizes the system relationship as obtained from the observed data (Wigley et al., 1990). Statistical downscaling can be classified into three different types. One is transfer function-based methods (Wigley et al., 1990; Buishand et al., 2004; Ghosh and Mujumdar, 2008), which represents whether the relationship is linear or non-linear between the predictor and predictand. Next is the weather pattern-based approach (Schnur and Lettenmaier, 1998; Kidson and Renwick, 2002), which includes the grouping of local meteorological variables with various classes of the atmospheric circulation, and the last is stochastic weather generators (Wilks, 1998; Khalili et al., 2009) that gives synthetic time series of the weather data for infinite length by using statistical properties of the observed weather in a particular location. Various methods are used widely for the statistical downscaling (Chu et al., 2010) among which Support Vector Machine (SVM) is an important method used by many researchers (Anandhi et al., 2009; Raje and Mujumdar, 2011). A recent study of the climate change was done in Sikkim of India indicating effect of temperature and rainfall change on crop yield (Deb et al., 2014).

As observed from the above study, although future generations of rainfall and temperature is frequent, but there has been limited study of future generation of evapotranspiration. However, evapotranspiration is not only major climatic parameters controlling water balance, but also a major factor controlling crop production. And in the areas of limited rainfall or rainfall based agricultural season (as in the case of study area), variation in ET may create problem. In this area, which is situated in the central India in Narmada river basin, future generation of evapotranspiration has not been done before. It is also necessary to correlate three parameters and to assess their effects in the future to develop better management strategies. Therefore, the major objectives are (1) to downscale future climate parameters (rainfall, temperature) and to assess its impact in the study area; (2) and to estimate future reference evapotranspiration (ET_0) from the downscaled temperature by Hargreaves method in three stations in the study area, which also shows a relation to the temperature variation of the area. The study has been carried out with the GCM (HADCM3) data downscaled with Least Square Support Vector Machine (LS-SVM) model.

2. Study area

The study area is located in the central part of India and is a part of the Narmada River basin in Madhya Pradesh. The area extends from 21°47′24″N to 23°26′06″N and 77°34′44″E to 78°42′21″E with the total area of 12,290 km^2. It covers three districts of Betul, Hoshangabad and Raisen. The region experiences the subtropical type of climate with hot, dry summer from April to June and a cool dry winter. The average rainfall varies from 900 to 1150 mm annually as observed in the last 41 years of rainfall data. Maximum rainfall (more than 80%) occurs during the monsoon season. Annual minimum and maximum temperatures vary from 19.5 to 32.5 °C (last 41 years temperature data) (Fig. 1).

3. Data and methodology

3.1. Data

The monthly observed rainfall, minimum temperature and maximum temperature data have been taken for 3 stations for 41 years (1961–2001) from the Indian Water Portal. The outliers within the data series were checked and the detected values were computed with the use of the normal ratio method. Future ET_0 is calculated from the downscaled temperature data by the Hargreaves method (Hargreaves and Samani, 1982) due to limited data availability. Details of the stations are given in the Table 1.

HADCM3 and NCEP (National Center for Environmental Prediction) data have been used for future prediction with the A2 scenario obtained from the given link (http://www.cccsn.ec.gc.ca/?page=pred-hadcm3).

3.2. Methodology

The predictor data have been obtained from the NCEP for 41 years from 1961 to 2001 (Kalnay et al., 1996) on the scale of 2.5° (latitude) × 2.5° (longitude). Proper selection is required for the predictors for downscaling and the selected variables should be simulated by GCMs which remain correlated with the surface variables (Wetterhall et al., 2005). The monthly variables (rainfall, minimum and maximum temperature) have been used to downscale the predicted future climate with the HADCM3 model (Hadley GCM 3). It has a grid dimension of 2.5° latitude × 3.75° longitude (417 km × 278 km area). According to Toews and Allen (2009), HADCM3 is considered as very popular and mature model and many studies are found with this model (Houghton et al., 2001; Collins et al., 2001; Hassan et al., 2013). Analysis was done with the A2 scenario with the model output of 1961 to 2099. The NCEP grid points and HADCM3 grid points' locations do not match, thus inverse distance weighted method (IDW) of interpolation was applied prior to the use of GCM outputs in prediction.

The NCEP Reanalysis data are provided by the NOAA-CIRES Climate Diagnostics Center, Boulder, Colorado, USA. The NCEP/NCAR Reanalysis Project is a joint project between the National Centers for Environmental Prediction (NCEP) and the National Center for Atmospheric Research (NCAR). The main objective of this joint effort is to provide new atmospheric analyses using historical

Please cite this article in press as: Kundu, S., et al., Future changes in rainfall, temperature and reference evapotranspiration in the central India by Least Square Support Vector Machine, Geoscience Frontiers (2016), http://dx.doi.org/10.1016/j.gsf.2016.06.002

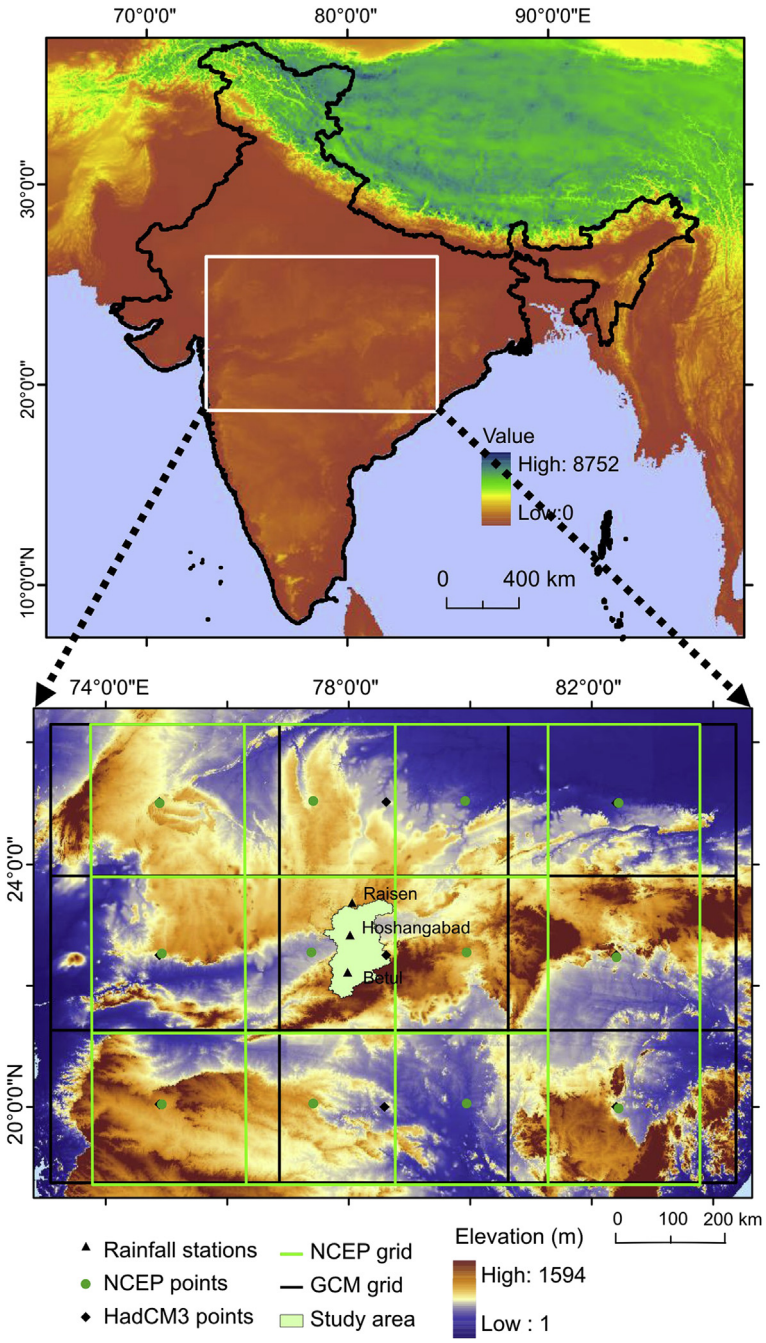

Figure 1. Study area.

data (1957 onwards) and to give analyses of the current atmospheric state (Climate Data Assimilation System, CDAS). The NCEP data is applied to generate the GCM outputs (example HADCM3) for the entire globe. However, the resolution of the NCEP data is 2.5° × 2.5° (latitude × longitude) grid. The NCEP/NCAR Reanalysis 1 version is used for the study. The link is http://www.esrl.noaa.gov/psd/data/gridded/data.ncep.reanalysis.html.

The observed station data have been taken as predictands with the NCEP (predictor) variable from 1961 to 2001 for annual climatic analysis. Among 26 variables of the NCEP data, only highly correlated data have been selected as the predictors (Table 2). The selected NCEP data are then standardized. The LS-SVM model is performed for calibration and validation using selected predictor of NCEP and observed data. During the calibration and validation time, 70% (1961–1989) and 30% (1990–2001) of data sets have been used respectively. Predictor selection is an essential process for downscaling and it is said that a variable can be considered as a predictor if there exist a relationship between the predictor and the predictand (Wetterhall et al., 2005). Selection of predictors is done on the basis of some factors such as (1) majority of predictors should remain physically related to the local-scale elements and should be realistically GCM simulated, (2) predictors should be available from the datasets and output archives of GCM, (3) remain highly correlated to the predicted data. Raje and Mujumdar (2011) selected the predictors for the SVM method based on the screening of the predictor variables at the beginning by analyzing the correlation with the downscaled variable at one station. Similar methods have been applied in this research.

Please cite this article in press as: Kundu, S., et al., Future changes in rainfall, temperature and reference evapotranspiration in the central India by Least Square Support Vector Machine, Geoscience Frontiers (2016), http://dx.doi.org/10.1016/j.gsf.2016.06.002

Table 1
Information of stations.

Sl no.	Station name	Lat. (°N)	Long. (°E)	Alt (m)	Duration of data	Data type
1	Betul	21.18	78.06	437	1961–2001	Rainfall, Minimum and maximum temperature and ET_0 estimated from temperature
2	Hoshangabad	22.73	78.08	313	1961–2001	
3	Raisen	23.26	78.12	433	1961–2001	

Table 2
Selected predictor variables.

Sl no.	Predictors	Full name of predictors	Rainfall	T_{max}	T_{min}
1	Mslp	Mean sea level pressure	Yes	Yes	Yes
2	p__u	Zonal velocity component		Yes	Yes
3	p__v	Meridional velocity component		Yes	Yes
4	p__z	Vorticity (surface)	Yes	Yes	Yes
5	p500	Geopotential height at 500 hPa	Yes	Yes	Yes
6	p850	Geopotential height at 850 hPa	Yes		
7	temp	Mean temperature		Yes	Yes
8	p5zh	Divergence at 500 hP			
9	p5th	Wind direction at 500 hPa			
10	rhum	Surface relative humidity	Yes		
11	shum	Specific humidity	Yes		
12	r500	Relative humidity at 500 hPa			
13	r850	Relative humidity at 850 hPa			
14	p5_v	Zonal wind at 500 hPa	Yes		
15	p5_z	Vorticity at 500 hPa	Yes		
16	p8_z	Vorticity at 850 hPa	Yes		
17	p8_th	Wind direction at 850 hPa	Yes		

The reduced climate variable signifies a major portion of the variability within the original data. The LS-SVM method has been used on the reduced standardized data and calibration and validation is performed. The GCM (or HADCM3 here) data have been standardized before using it. The trained LS-SVM model is analyzed to get downscaled future rainfall and temperature outputs. Bias correction is applied to the predicted data. The LS-SVM model used to obtain downscaled future rainfall and temperature projection of the A2 scenario of three stations, are presented in decade outputs from 2011 to 2099. The future ET_0 is then generated from the downscaled temperature for the period of 2011 to 2099 (Fig. 2).

3.2.1. LS-SVM method

Least Square Support Vector Machines (LS-SVM) is considered to have few advantages over the standard SVM (Suykens, 2001). LS-SVM is a least square version of the standard SVM and has a kernel-based method.

Here, a linear solution corresponds to the non-linear solution in the higher dimensional feature space to the lower dimensional input space respectively. This helps SVM in downscaling the non-linear problems (Anandhi et al., 2008). Instead of the convex quadratic programming (QP) problem for the standard SVM, solve of linear equations are carried out in LS-SVM. LS-SVM is proposed by Suykens and Vandewalle (1999) and has been used in the works of Tripathi et al., (2006) and Anandhi et al., (2008) for the downscaling of rainfall. N patterns $\{(x_i, y_i), i = 1,\ldots, N\}$ of a finite training sample are considered, where x_i stands for the ith pattern in the N-dimensional space ($x_i = [x_{1i},\ldots, x_{Ni}] \in \Re^N$) form input to the LS-SVM, and where $y_{Yi} \in \Re^N$ represents the corresponding value of the required output of the model. Again, by considering learning machine by a set of possible mappings, $x \mapsto f(x, w)$, where $f(\cdot)$ denotes a deterministic function that always provides the same output for the given input pattern x parameters w ($w \in \Re^N$). The training phase of the learning machine includes adjustment of the parameters w. Parameter estimation is made by minimizing the cost function $\Psi_L(w \in \Re^N)$. The optimization problem of LS-SVM for estimation of the function is made by minimization of the cost function.

$$\Psi_L(w, e) = \frac{1}{2}w^T w + \frac{1}{2}C\sum_{i=1}^{N} e_i^2 \tag{1}$$

3.3. Subject to the constraint of equality

$$y_i - \hat{y}_i = e_i \;\; i = 1, \ldots\ldots, N \tag{2}$$

where C represents a positive real constant and $\hat{y}$ shows the actual model output. The initial term of the cost function denotes model complexity-penalty function or weight decay. This function is used to regularize the weight sizes and to penalize the large weights. Hence, this helps in the improvement of generalization performance (Hush and Horne, 1993). The next or the second term of the cost function gives the penalty function. The optimization problem solution is attained by considering the Lagrangian given as

$$L(w, b, e, \alpha) = \frac{1}{2}w^T w + \frac{1}{2}C\sum_{i=1}^{N} e_i^2 - \sum_{i=1}^{N}\alpha_i\{\hat{y}_i + e_i - y_i\} \tag{3}$$

where α_i represents the Lagrange multipliers and b denotes the bias term. The optimality conditions are given by

$$\begin{cases} \dfrac{\partial L}{\partial w} = w - \sum_{i=1}^{N}\alpha_i\phi(x_i) = 0 \\ \dfrac{\partial L}{\partial b} = \sum_{i=1}^{N}\alpha_i = 0 \\ \dfrac{\partial L}{\partial e_i} = \alpha_i - Ce_i = 0, i, \ldots\ldots, N \\ \dfrac{\partial L}{\partial \alpha_i} = \hat{y}_i + e_i - y_i = 0, i = 1, \ldots\ldots, N \end{cases} \tag{4}$$

The conditions above of optimality can be given as the solution to the following set of linear equations after eliminating w and e_i

$$\begin{bmatrix} 0 & \rightarrow 1^T \\ \rightarrow 1 & \Omega + C^{-1}I \end{bmatrix}\begin{bmatrix} b \\ \alpha \end{bmatrix} = \begin{bmatrix} 0 \\ y \end{bmatrix} \tag{5}$$

where,

$$y = \begin{bmatrix} y_1 \\ y_2 \\ \vdots \\ y_N \end{bmatrix}; \vec{1} = \begin{bmatrix} 1 \\ 1 \\ \vdots \\ 1 \end{bmatrix}_{N\times N} \tag{6}$$

$$\alpha = \begin{bmatrix} \alpha_1 \\ \alpha_2 \\ \vdots \\ \alpha_N \end{bmatrix}; I = \begin{bmatrix} 1 & 0 & \cdots & 0 \\ 0 & 1 & \cdots & 0 \\ \vdots & \vdots & \vdots & \vdots \\ 0 & 0 & \cdots & 1 \end{bmatrix}_{N\times N} \tag{7}$$

Here I_N represents $N \times N$ identity matrix, and $\Omega \in R^{N\times N}$ represents the kernel matrix defined by Ω that has been obtained from the application of Mercer's theorem.

$$\Omega_{i,j} = K(x_i, x_j) = \varphi(x_i)^T\varphi(x_j)\ldots\forall i, j \tag{8}$$

where $\varphi(\cdot)$ is the nonlinear transformation function that converts a nonlinear problem to the linear problem in a feature space of higher dimension. The resulting LS-SVM model for estimation of function is given as

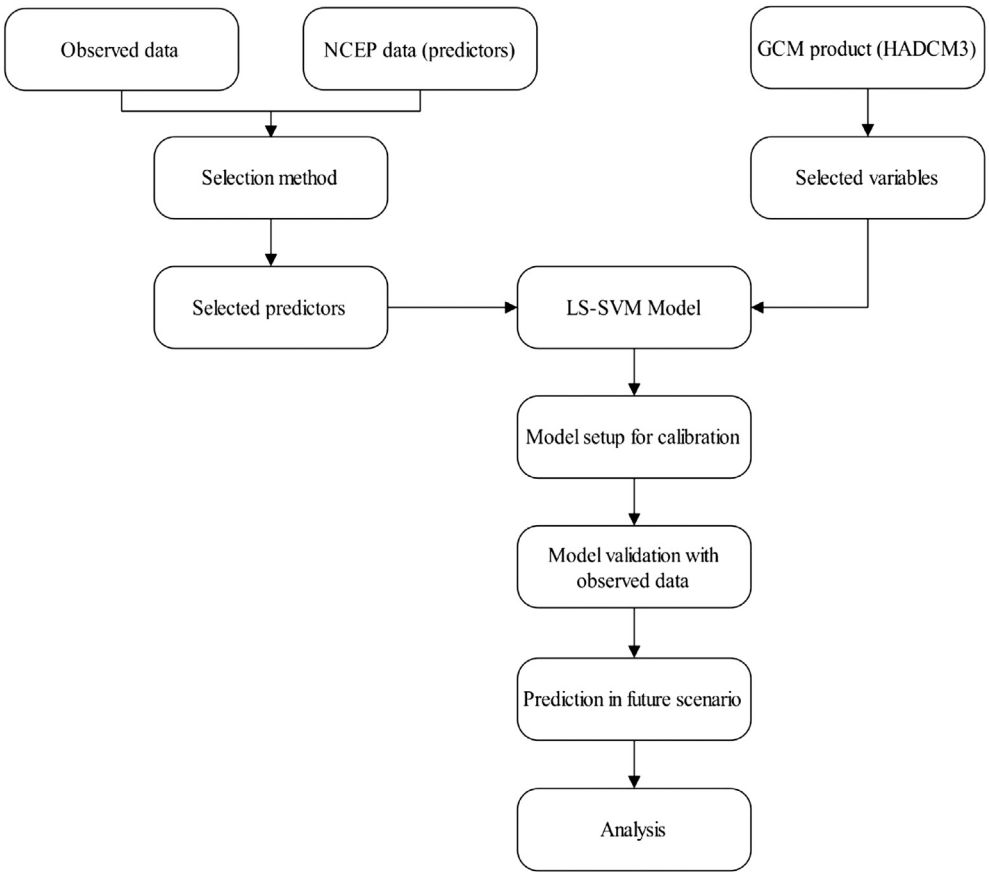

Figure 2. Methodology.

$$f(x) = \sum \alpha_i^* K(x_i, x) + b^* \quad (9)$$

where, $K(x_i, x)$ is considered as the inner product kernel function (product of vectors x_i and x_j) which is defined in accordance with Mercer's theorem (Mercer, 1909; Courant and Hilbert, 1970) and b^* represents the bias. Various kernel functions are found including linear, polynomial, splines, sigmoid and radial basis function (RBF) from which Radial basis function (RBF) method is used here. The linear kernel is considered as a special case of the RBF (Keerthi and Lin, 2003). In this case RBF is used which is given as,

$$K(x_i, x_j) = \exp\left(-\frac{\|x_i - x_j\|^2}{2\sigma^2}\right) \quad (10)$$

where, σ represents the width of RBF kernel that can be adjusted for the control of the RBF expressivity. The RBF kernels show finite and localized responses across the entire range of predictors.

3.3.1. Bias correction of the predictands

The LS-SVM model used to obtain future rainfall projection of the A2 scenario, are given as the projected rainfall, minimum and maximum temperatures and ET_0 of every decade from 2011 to 2099 (2011–2020, 2021–2030, 2031–2040, 2041–2050, 2051–2060, 2061–2070, 2071–2080, 2081–2090 and 2091–2099) of three stations of Betul, Hoshangabad and Raisen. Bias correction was applied to the predicted data. The use of non-linear method was done for the correction by a power law relationship of $P^* = aP^b$, where a and b are constants. This method is not used for bias correction of the normally distributed data, because this method produces a dataset that is not normally distributed. The adjustment of mean and variance is performed in the correction. It is given as (Leander and Buishand, 2007),

$$P_{SDcorr} = \overline{P}_{obs} + \left(\frac{\sigma(P_{obs})}{\sigma(P_{gcm})}\right) \times \left(P_i - \overline{P_{obs}}\right) + \left(\overline{P_{obs}} - \overline{P_{gcm}}\right) \quad (11)$$

where, P_{SDcorr} is the climatic variables with bias correction; $\overline{P}_{obs}$ is the mean daily observed climatic variables; $\overline{P}_{gcm}$ represents the mean daily GCM climatic variables (predicted); $\sigma(P_{obs})$ is the standard deviation showing the observed climate variables; $\sigma(P_{gcm})$ stands for the standard deviation of the GCM climate variables (predicted); P_i represents the daily or monthly climate variables from HadCm3 data (not corrected). This method of bias correction was used by Raneesh and Thampi (2013) and Mondal et al. (2014).

3.3.2. LS-SVM performance

The LS-SVM model calibration and validation is assessed by four performance indexes used by other researchers such as, Root mean square error (RMSE) (Kundu et al., 2014), Normalized Mean Square error (NMSE) and Nash-Sutcliffe coefficient (NASH) and correlation coefficient (CC) (Duhan and Pandey, 2014; Nash and Sutcliffe, 1970).

Root mean square error is given as

$$RMSE = \sqrt{\frac{1}{N}\sum_{i=1}^{N}\left(y_i - \hat{y}_i\right)^2} \quad (12)$$

Please cite this article in press as: Kundu, S., et al., Future changes in rainfall, temperature and reference evapotranspiration in the central India by Least Square Support Vector Machine, Geoscience Frontiers (2016), http://dx.doi.org/10.1016/j.gsf.2016.06.002

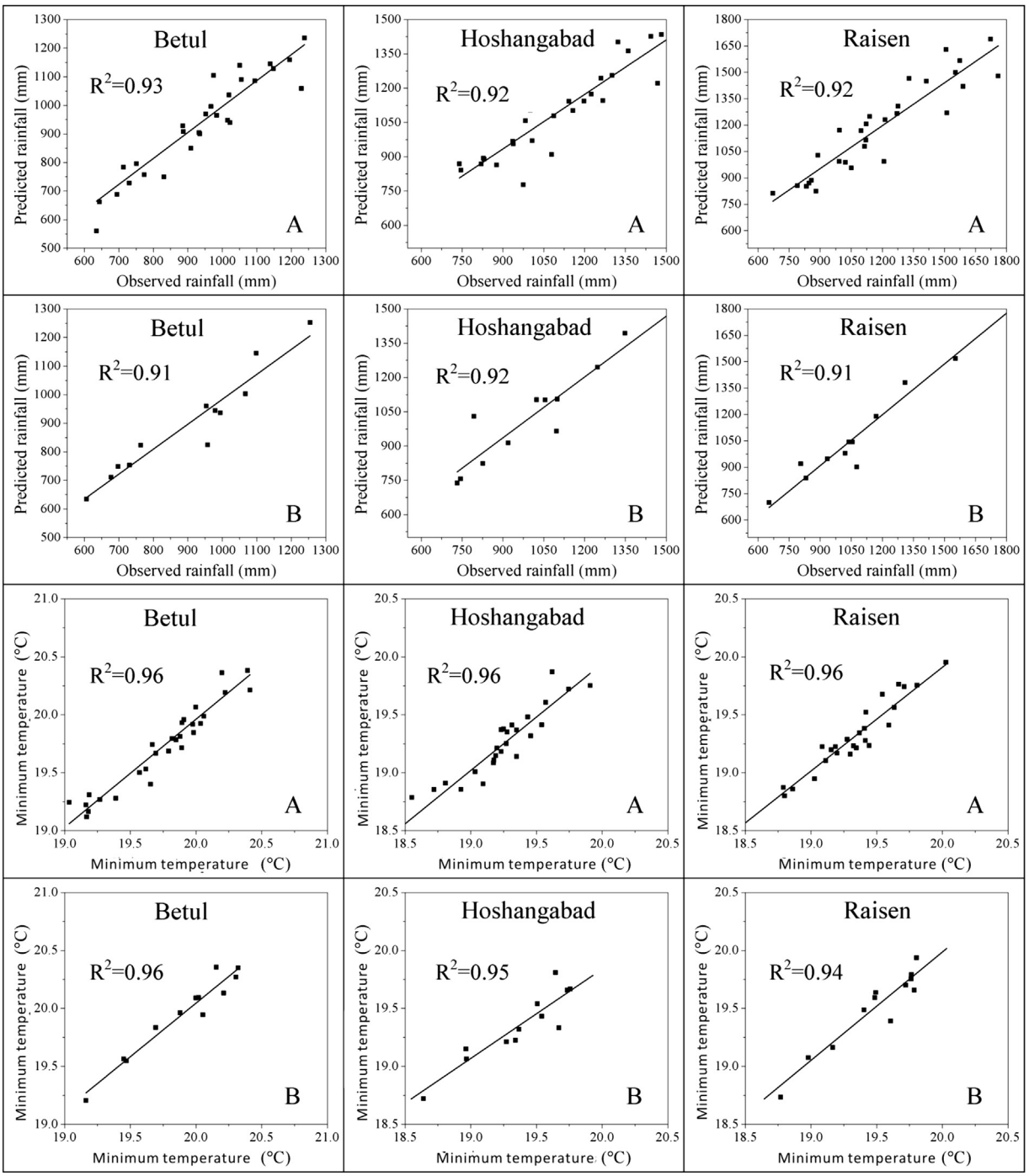

Figure 3. Calibration and Validation of LS-SVM of different variables (rainfall, minimum temperature, maximum temperature and ET_0).

$$\text{Normalized Mean Square error is NMSE} = \frac{\frac{1}{N}\sum_{i=1}^{N}\left(y_i - \widehat{y}_i\right)^2}{(S_{\text{obs}})^2} \quad (13)$$

$$\text{Nash} - \text{Sutcliffe coefficient is NASH} = 1 - \frac{\frac{1}{N}\sum_{i=1}^{N}\left(y_i - \widehat{y}_i\right)^2}{\frac{1}{N}\sum_{i=1}^{N}\left(y_i - \widehat{y}_i\right)^2} \quad (14)$$

Please cite this article in press as: Kundu, S., et al., Future changes in rainfall, temperature and reference evapotranspiration in the central India by Least Square Support Vector Machine, Geoscience Frontiers (2016), http://dx.doi.org/10.1016/j.gsf.2016.06.002

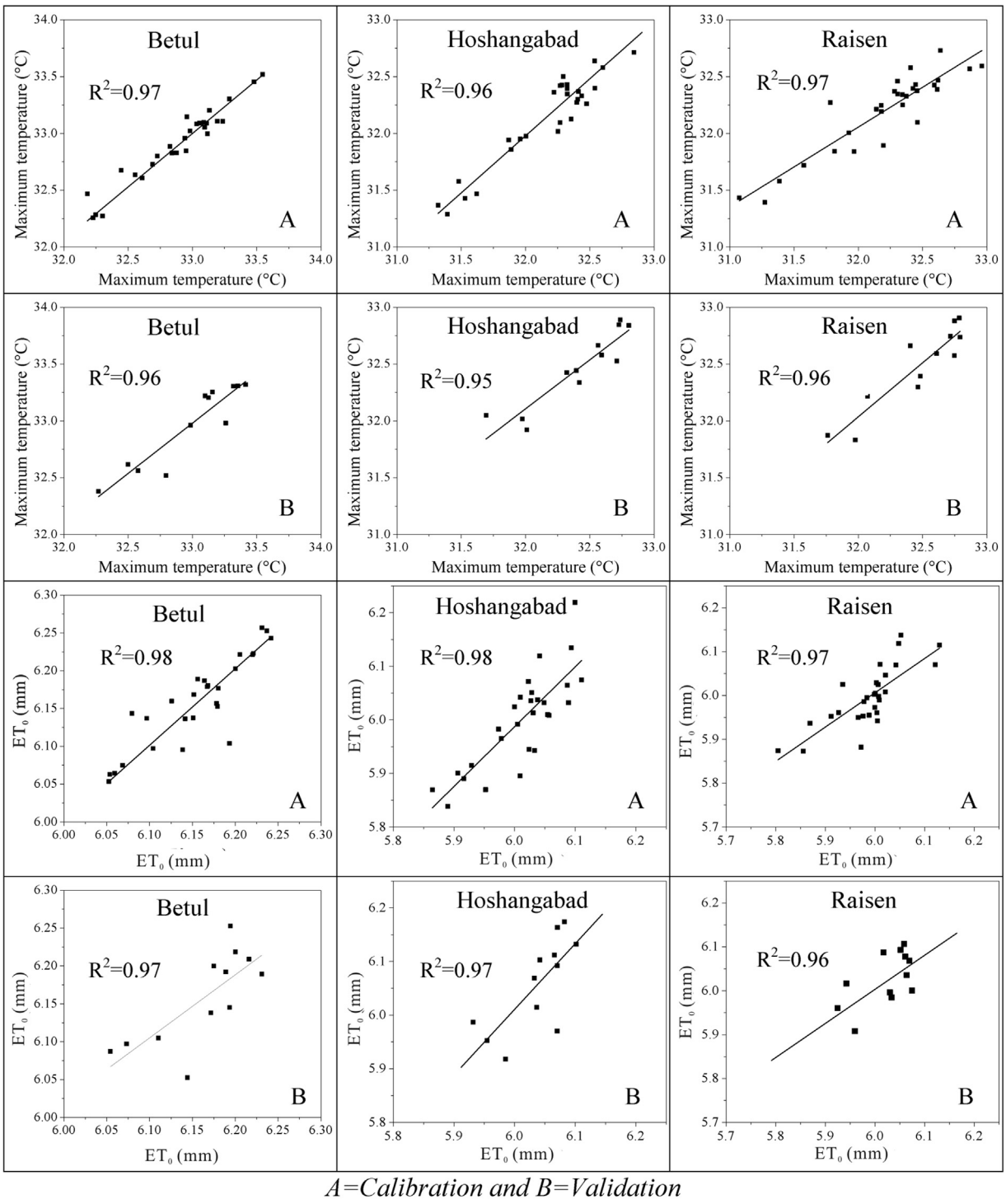

Figure 3. *(Continued)*

Correlation coefficient CC

$$= \frac{N\sum\left(y_i - \hat{y}_i\right) - (\sum y_i) \times \left(\sum \hat{y}_i\right)}{\sqrt{\left[N\sum\left(y_i - \hat{y}_i\right)^2\right] \times \left[N\sum\left(y_i - \hat{y}_i\right)^2\right]}} \quad (15)$$

Where, y_i and $\hat{y}_i$ show the time series of the observed and simulated predictands respectively and the N represents the sample size of the training and testing data. A small value of the RMSE and NMSE depicts that the discrepancy is less between the observed and predicted series; hence it will provide better accuracy for prediction while in case of NASH and CC the higher values give better accuracy.

The reference evapotranspiration or ET_0 has been calculated using the Hargreaves method from the downscaled temperature data. It is given as (Hargreaves and Samani, 1985; Vicente-Serrano et al., 2014),

Please cite this article in press as: Kundu, S., et al., Future changes in rainfall, temperature and reference evapotranspiration in the central India by Least Square Support Vector Machine, Geoscience Frontiers (2016), http://dx.doi.org/10.1016/j.gsf.2016.06.002

Table 3
Model performance at calibration and validation time.

	Betul		Hoshangabad		Raisen	
Methods	Calibration	Validation	Calibration	Validation	Calibration	Validation
Rainfall						
RMSE	15.911	16.273	16.253	27.053	13.469	19.148
NMSE	2.254	2.503	1.885	5.429	1.139	2.351
NASH	0.950	0.946	0.958	0.952	0.952	0.950
CC	0.962	0.954	0.961	0.957	0.958	0.953
Minimum Temperature						
RMSE	1.35	1.51	0.98	1.12	1.44	1.57
NMSE	0.98	1.12	0.054	0.069	0.076	0.084
NASH	0.968	0.961	0.975	0.96	0.969	0.965
CC	0.981	0.978	0.982	0.973	0.978	0.971
Maximum Temperature						
RMSE	0.95	1.12	0.81	0.96	1.22	1.36
NMSE	0.073	0.087	0.056	0.069	0.091	0.119
NASH	0.97	0.967	0.971	0.964	0.973	0.97
CC	0.985	0.981	0.979	0.976	0.986	0.979
ET_0						
RMSE	0.104	0.203	0.106	0.188	0.146	0.177
NMSE	0.007	0.027	0.007	0.022	0.013	0.019
NASH	0.985	0.983	0.986	0.981	0.981	0.979
CC	0.989	0.985	0.989	0.986	0.985	0.982

$$ET_0 = 0.0023 R_a TD^{0.5}(T + 17.8) \quad (16)$$

Here, R represents the Linacre equation, R_a stands for the extraterrestrial solar radiation, T is mean air temperature, and TD shows the difference between maximum and minimum temperature.

4. Results and discussion

4.1. Model calibration and validation

For developing the SVM model, 70% of the data were used for calibration and remaining 30% of the data were used for validation of the model. The three stations of Betul, Hoshangabad and Raisen were used for the downscaling. The training data was taken from 1961–1989 and 1990–2001 were used in the testing of the dataset. The data of rainfall and temperature were used as the predictand. Fig. 3 shows the observed and predicted monthly rainfall, minimum and maximum temperature and ET_0 for the calibration and validation of LS-SVM model of Betul, Hoshangabad and Raisen. It can be deduced from the given graph that the predicted values of the validation are very close to the observed values for all the three stations. Calibration also has given quality result between the observed and predicted values.

4.2. Model efficiency

In order to obtain good results between the observed and predicted variable, the parameters of the model are adjusted at the time of calibration with different statistical measures for performance, such as Root Mean Square Error (RMSE), Normalized Mean square Error (NMSE), Nash–Sutcliffe Efficiency Index (NASH) and Correlation Coefficient (CC). The calibrated and validated errors of LS-SVM model of three stations of the study area are given in the Table 3. In rainfall, the calibrated values of the RMSE range from 13.47 to 16.25 m and validation ranges from 16.27 to 27.05 m. NMSE ranges from 1.14 to 2.25 m for calibration and 2.35 to 5.43 m for validation. The NASH values vary from 0.950 to 0.958 (calibration) and from 0.950 to 0.956 (validation). The CC values range from 0.958 to 0.962 for calibration and from 0.953 to 0.957 for validation. In minimum temperature, the RMSE varies from 0.98 to 1.44 m in calibration and 1.12 to 1.57 m in validation. In NMSE, the calibrated values vary from 0.054 to 0.076 m and validation values range from 0.069 to 0.084 m. The Nash values vary from 0.968 to 0.975 (calibration) and from 0.96 to 0.965 (validation). In CC, calibration values range from 0.978 to 0.982 and validation ranges from 0.971 to 0.978. In maximum temperature, the RMSE values for calibration range from 0.81 to 1.22 m and validation from 0.96 to 1.36 m. In NMSE, the calibration varies from 0.056 to 0.091 m and validation varies from 0.069 to 0.119 m. In NASH, calibration ranges from 0.97 to 0.973 and validation from 0.964 to 0.97. In CC, calibration varies from 0.979 to 0.986 and validation from 0.976 to 0.981. The ET_0 accuracy in RMSE varies from 0.104 to 0.146 m (calibration) and from 0.177 to 0.203 m (validation). The NMSE values of calibration range from 0.007 to 0.013 m and validation from 0.019 to 0.027 m. The Nash values of LS-SVM vary from 0.981 to 0.986 (calibration) and from 0.979 to 0.983 (validation) and the CC values of calibration vary from 0.985 to 0.989 and validation from 0.982 to 0.986. ET_0 accuracy results also indicate good performance of the LS-SVM model (Table 3).

4.3. Downscale of future projected rainfall, minimum temperature, maximum temperature and calculated ET_0 of the A2 scenario

Downscaling of the A2 scenario, as simulated from the GCM, is performed after the calibration and validation of the LS-SVM model. The GCM (HADCM3) data are used in the calibrated and validated LS-SVM model to obtain a downscaled result of future projected predictands or annual rainfall, ET_0, minimum and maximum temperatures. This is illustrated by the box diagram in Fig. 4 for the time slices of 10 years from 2011 to 2099 (2011–2020, 2021–2030, 2031–2040, 2041–2050, 2051–2060, 2061–2070, 2071–2080, 2081–2090 and 2091–2099) of the three stations of Betul, Hoshangabad and Raisen. The middle line of the box plot represents the median value while the upper and lower edges signify the 75% and the 25% of the data set respectively. The highest and lowest limits of the upper and lower vertical lines indicate highest and lowest values respectively. The black square depicts the simulated mean and the pink straight line shows the observed mean from 1961 to 2001. The data downscaled with the NCEP and the GCM data are compared with the observed data. This figure show an increase in the future rainfall, temperatures and ET_0 with some fluctuations of increase and decrease within decades.

Please cite this article in press as: Kundu, S., et al., Future changes in rainfall, temperature and reference evapotranspiration in the central India by Least Square Support Vector Machine, Geoscience Frontiers (2016), http://dx.doi.org/10.1016/j.gsf.2016.06.002

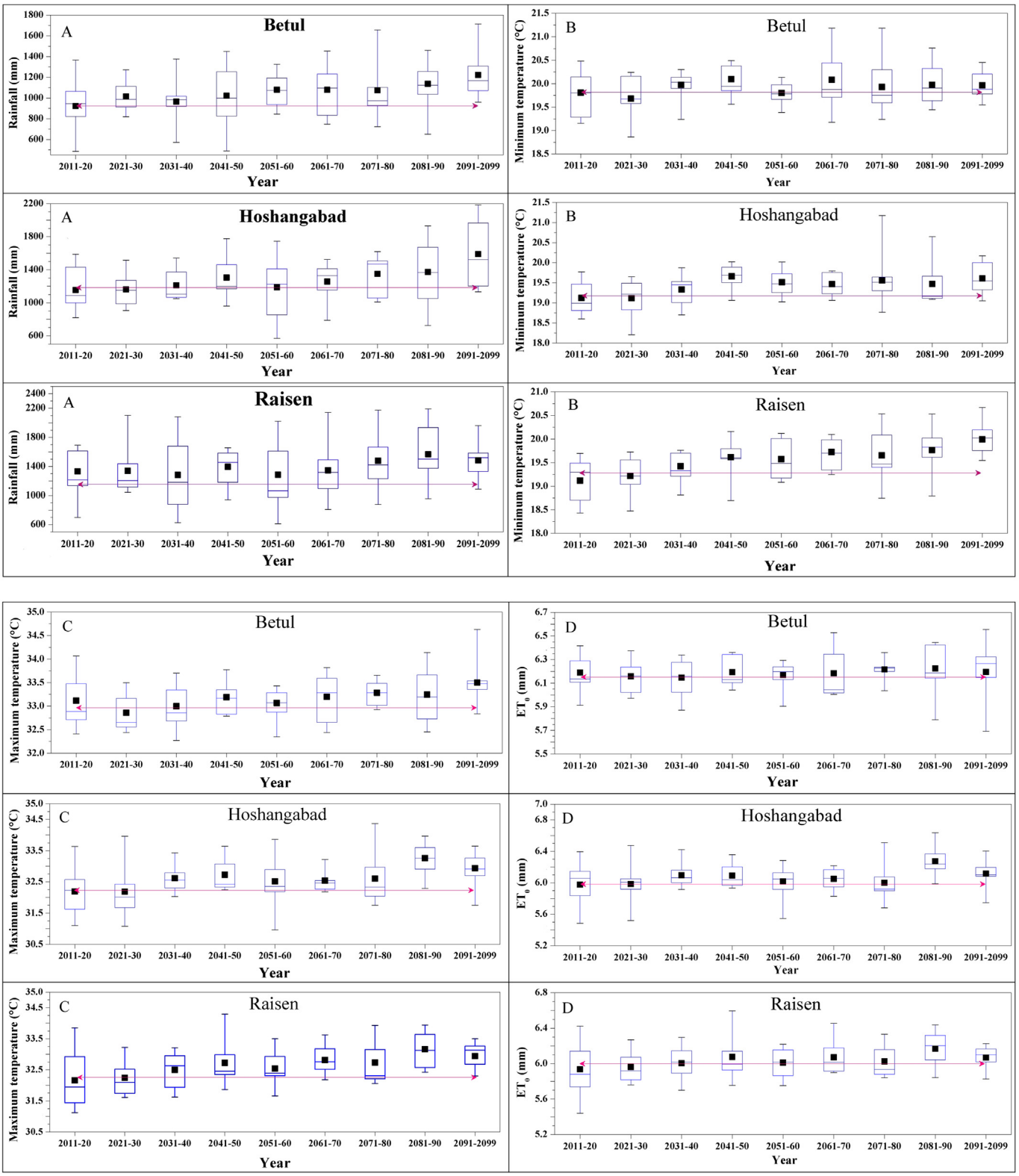

Figure 4. Future scenario of different decades (A) Rainfall, (B) minimum temperature, (C) maximum temperature, and (D) ET_0.

4.3.1. Rainfall

Increasing rainfall is observed in all the three stations compared to the observed mean value of 926.93 mm. In Betul, 2011–2020 indicates very similar mean to the observed rainfall. There is a continuous rising trend with little fluctuation in 2031–2040 and 2071–2080. The decade of 2091–2099 shows the highest increase (approx. >1200 mm). Hoshangabad experiences a little higher observed mean of 1088.85 mm than Betul that increases to around

Please cite this article in press as: Kundu, S., et al., Future changes in rainfall, temperature and reference evapotranspiration in the central India by Least Square Support Vector Machine, Geoscience Frontiers (2016), http://dx.doi.org/10.1016/j.gsf.2016.06.002

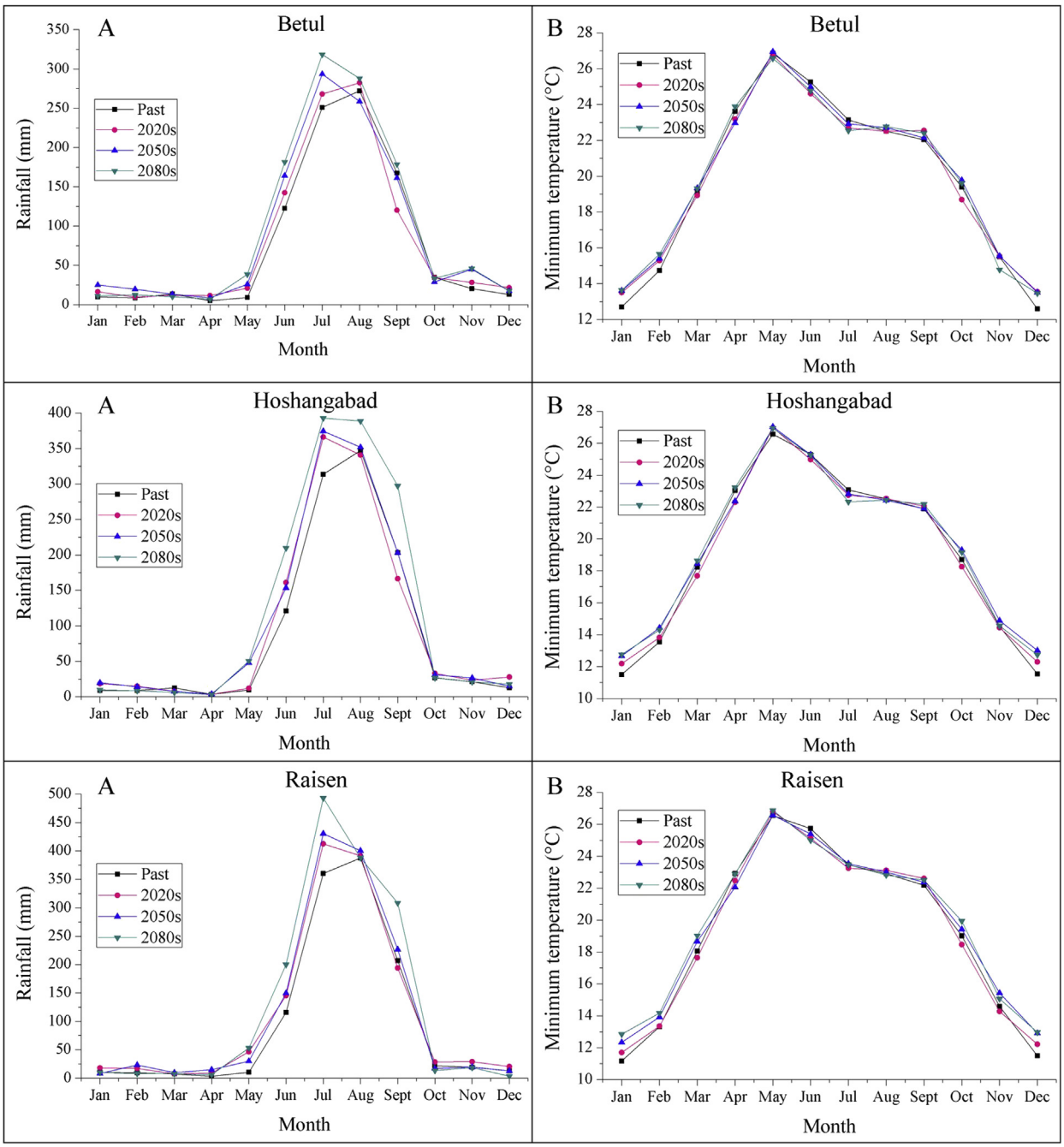

Figure 5. Future scenario of different months (A) Rainfall, (B) minimum temperature), (C) maximum temperature, and (D) ET_0.

1600 mm in 2091–2099. There is little fluctuation with downward trend in the 2021–2030 and 2051–2060 but the overall trend is showing an increase in the future rainfall. Raisen experiences the mean observed rainfall of 1165.88 mm and all the future rainfall shows an increase than the observed mean. Highest increase is observed in the 2081–2090 (approx. 1600 mm) that decreases to about 1500 mm in the 2091–2099 (Fig. 4A,B).

4.3.2. Minimum temperature

There is an increase in the simulated mean of minimum temperature in the future than the observed mean. In Betul, the observed mean is 19.8 °C and the simulated mean of 2011–2020 and 2051–2060 is similar to the observed mean. The period of 2061–2070 indicates highest rise in the minimum temperature (>20 °C) and an overall increasing temperature is noticed in all the decades with few ups and downs. In Hoshangabad, the mean observed temperature is 19.2 °C showing an increasing temperature from 2021–2030 onwards. Highest increase is observed in the 2041–2050 (around 19.6 °C). The increase is also high in the 2091–2099. In Raisen, the mean observed minimum temperature is 19.3 °C and there is an almost gradual increasing trend from 2011–2020 onwards. The 2011–2020 and 2021–2030 indicate a

Please cite this article in press as: Kundu, S., et al., Future changes in rainfall, temperature and reference evapotranspiration in the central India by Least Square Support Vector Machine, Geoscience Frontiers (2016), http://dx.doi.org/10.1016/j.gsf.2016.06.002

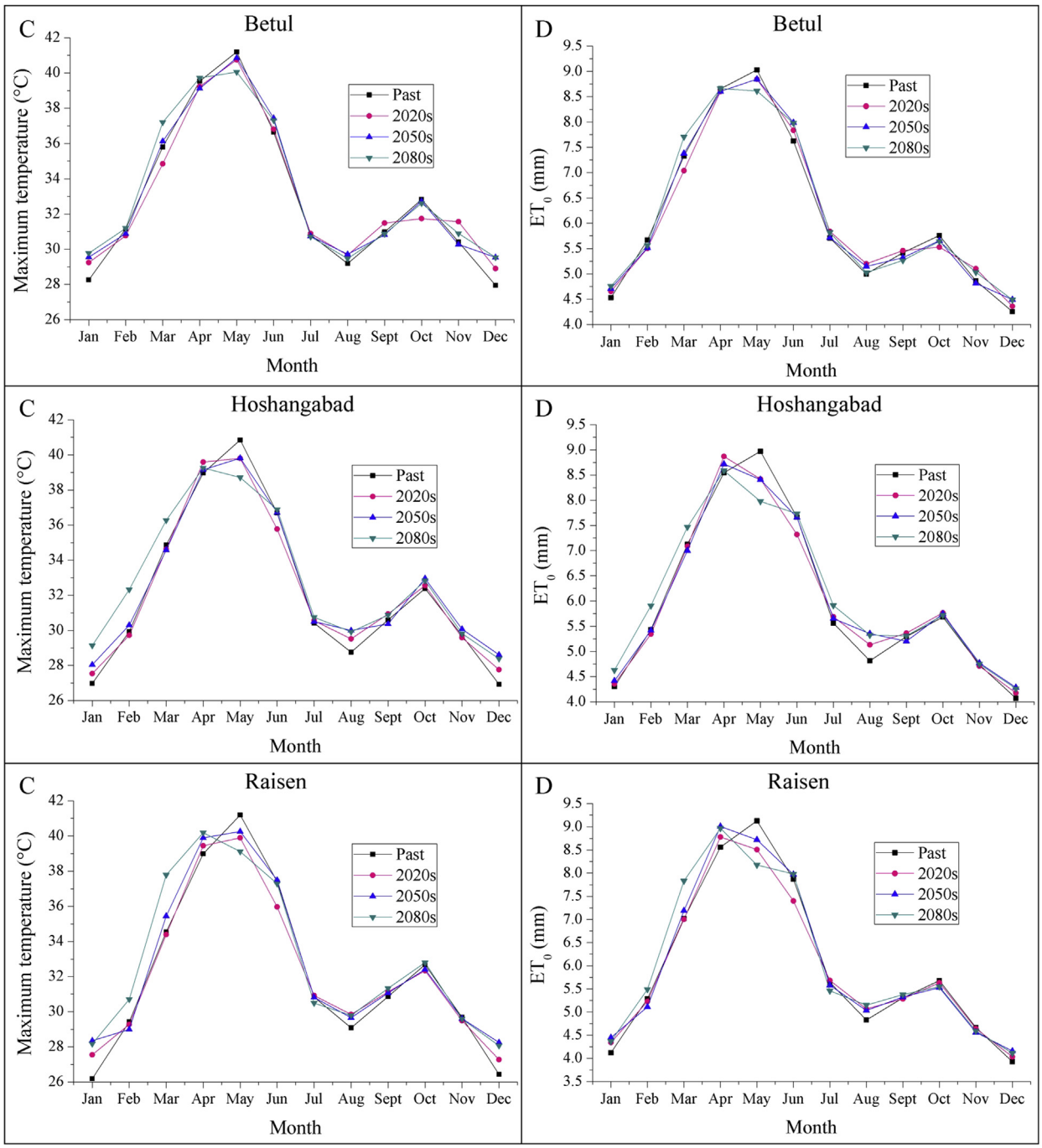

Figure 5. (*continued*).

lower temperature than the observed mean. The highest temperature increase is observed in the year 2091–2099 (approx. 20 °C) (Fig. 4A,B).

4.3.3. Maximum temperature

The maximum temperature is projecting a continuous increase in the future in the three stations. The observed mean of Betul is 32.9 °C. The decade of 2021–2030 shows that the simulated mean is less than the observed mean, but there is a constant increase from the 2030 onwards. The highest increase is observed in the 2091–2099 (33.5 °C). Hoshangabad indicates the mean observed maximum temperature of 32.3 °C with the highest increase in the 2091–2099 (33.2 °C). The initial decades show decrease up to the year 2030 and there is a continuous increase in the simulated temperature after that. Raisen has the mean observed temperature of 32.3 °C and 2081–2090 shows the maximum increase (33.2 °C). The temperature increase pattern in different decades is similar in Hoshangabad and Raisen. Hence, 2081–2090 and 2091–2099 have the highest rate of maximum temperature increase in three stations (Fig. 4C,D).

Please cite this article in press as: Kundu, S., et al., Future changes in rainfall, temperature and reference evapotranspiration in the central India by Least Square Support Vector Machine, Geoscience Frontiers (2016), http://dx.doi.org/10.1016/j.gsf.2016.06.002

4.3.4. Evapotranspiration (ET_0)

The ET_0 in all the three stations indicates a rise in different decades. The mean observed ET_0 of Betul is 6.15 mm and 2031–2040 shows lower simulated mean than the observed value. The decades of 2021–2040, 2041–2050 and 2051–2060 have almost similar ET_0 like the observed mean and highest increase is observed in 2081–2090. In Hoshangabad, the observed mean is 6.02 mm and the highest increase is in the 2081–2090. Some decades from 2011–2020, 2021–2030 and 2071–2080 have lower projected ET_0 values than the observed ET_0. Raisen experiences the observed mean ET_0 of 6 mm and highest is observed in 2081–2090 (6.16 mm). In Raisen also, in some decades from 2011–2040 and 2051–2060, lower simulated ET_0 than the observed value has been projected (Fig. 4C,D).

4.4. Downscale of future projected rainfall, minimum temperature, maximum temperature and calculated ET_0 of A2 scenario in different months

Fig. 5 gives the variation in the projected rainfall, minimum and maximum temperature and ET_0 respectively in different months as the mean of 30 years' time slice. Here, 2020s indicates the mean of 2011–2040, 2050s indicates mean of 2041–2070 and 2080s indicates mean of 2071–2099. The results of future rainfall are higher than the observed rainfall in all the three stations. The months of July and August (major monsoon months) show highest rainfall in three stations (Fig. 5A,B). The minimum temperature shows highest rise in May and June in the future in three stations. The winter months of December and January indicate a higher rate of increase in minimum temperature than other months (Fig. 5A,B). In case of monthly maximum temperature, there is a wide variation. Lower than the observed temperature is noticed in May while higher than the observed temperature is found in the December and January. The 2080s shows a higher rise in maximum temperature from February to April in all the stations. There are two peaks of the increase, one peak in April–May and then another small peak in October. This may occur as monsoon rains lower the day temperature and October indicates bright sunshine that might cause temperature rise (Fig. 5C,D). ET_0 is projecting a decrease in the future in May in three stations. Some decrease in different other months is also observed in three stations. Winter months show an increase in ET_0 in all the three stations (Fig. 5C,D).

There is a continuous rise in the minimum and maximum temperature. Some fluctuation with decreased temperature is found, but there is an overall increasing minimum and maximum temperatures generated by LS-SVM in the future. The ET_0 is a parameter that has been computed from temperature here, which is an indicative of the actual ET. Increasing temperature lead to the increase in the evapotranspiration or calculated ET_0 in most decades in all stations. Increased minimum temperature, particularly in the winter months is of significant concern indicating the global warming effect. Since Madhya Pradesh is a landlocked area, higher temperature projection in future might affect the cropping pattern and crop growth rate of the area. There is also an increase in the future rainfall. However, the increase in the rainfall will be a problem if very high intensity rainfall increases. Increasing minimum and maximum temperature of A2 scenario in the future is projected by Anandhi et al. (2009). A recent study in central India by Duhan and Pandey (2014) has shown an increase in the minimum and maximum temperature of the A2 scenario and has reported that LS-SVM has given the best result among three methods of multiple linear regression (MLR), artificial neural network (ANN) and Least Square Support Vector Machine (LS-SVM) for the future simulation of temperature. The LS-SVM is based on SVM method, which works and capture the non-linear relation between the predictand and the predictor (Raje and Mujumdar, 2011). The linear Statistical Downscaling Model (SDSM) and non-linear Support Vector Machine (SVM) have been compared and SVM model has given better results in downscaling precipitation with better basic statistics (Chen et al., 2010). Tripathi et al. (2006) showed that the SVM method is appropriate for precipitation downscaling at the regional scale and Anandhi et al. (2008) used the model at the basin scale. The present work is implementing the model at basin scale (12,290 km^2) and downscaling both precipitation and temperature and ET computation from the downscaled temperature. The methodology is observed to be strong in selecting the predictors which are chosen on the basis of their sensitivity to the rainfall and temperature. The calibration and validation results show the robustness of the model. The projected rainfall and temperature shows an increase in the future in different decades. An increasing temperature in India is also observed in the studies of Kothawale et al. (2012) and Rai et al. (2012). The increasing rate of future rainfall is observed in many works of India (Rupa Kumar et al., 2006), in the eastern (Kannan and Ghosh, 2011), north and northwest (Raje and Mujumdar, 2011) and south (Meenu et al., 2013) part of India. Increasing rainfall in a part of central India has also been reported by Mondal et al. (2014) in the A2 scenario. Increasing rate of ET_0 is reported by Rehana and Mujumdar (2013) in the southern part of India that also conforms to the present study. Increased ET_0 in the pre-monsoon season or in March to May months, when rainfall is very low and temperature increase is high, may require certain awareness and management strategies to cope with the situation.

5. Conclusion

The present study deals with the changes in the pattern of different climate variables to estimate and investigate the future changes in the water resources of the region. Three major parameters of climate, i.e. rainfall, temperature (minimum and maximum) and reference evapotranspiration have been considered to downscale the future projection of climate change over the basin area in the A2 scenario with the HADCM3 data. The ET is derived from the temperature only by the Hargreaves method, because of the non-availability of other parameters. Therefore, it does not include the sensitivity of other parameters affecting ET, as done by the Penman-Monteith method. However, according to the Vicente-Serrano et al. (2014), Hargreaves method can be considered as a quality technique in calculating ET_0 if all variables required for the Penman-Monteith are not available. The LS-SVM model is used for downscaling the GCM dataset to analyze the future climate from 2011 to 2099 in a part of the Narmada river basin of central India. The efficiency of the LS-SVM model is measured with four statistical methods (RMSE, NMSE, NASH, CC) in respect to model calibration and validation that proved the feasibility of the model. The results show an increase in the minimum and maximum temperatures in the A2 scenario in the future and 2081–2099 indicates a high increase. Winter months of December and January are affected by the highest change. The ET_0 is also projected to have increased with some fluctuation of both increase and decrease in different decades. Highest rise is projected in 2091–2099, particularly in the winter season (November to January) and the monsoon season (July to September). The resultant increase in rainfall is observed mainly in the monsoon months. The Hoshangabad and Raisen show a maximum increase in rainfall while Betul has the maximum ET_0. Although uncertainties are always there in the projection of climate change, but an estimation of the possible future changes in climate downscaled for an area is possible and essential. The increased rate of change may results in the occurrence of water related hazards or might create problems in the water availability. An increase in the

Please cite this article in press as: Kundu, S., et al., Future changes in rainfall, temperature and reference evapotranspiration in the central India by Least Square Support Vector Machine, Geoscience Frontiers (2016), http://dx.doi.org/10.1016/j.gsf.2016.06.002

future projection of all the parameters may imply future hazards of flood and drought occurrences. This study expresses the need for understanding the future change of climate that may lead to some accompanying changes in the local natural resources affecting the life of people.

Acknowledgment

The authors are thankful to the Water Portal for the rainfall data, to the Canadian Climate Data and Scenarios for providing the GCM and NCEP Data, and to the University Grant Commission (UGC) for providing financial assistance in this research.

References

Abbott, M.B., Bathurst, J.C., Cunge, J.A., O'Connell, P.E., Rasmussen, J., 1986. An introduction to the European hydrological system—systeme Hydrologique European 'SHE'. 1: history and philosophy of a physically based distributed modeling system. Journal of Hydrology 87 (1–2), 45–59.

Anandhi, A., Srinivas, V.V., Kumar, D.N., Nanjundiah, R.S., 2009. Role of predictors in downscaling surface temperature to river basin in India for IPCC SRES scenarios using support vector machine. International Journal of Climatology 29, 583–603.

Anandhi, A., Srinivas, V.V., Nanjundiah, R.S., Nagesh Kumar, D., 2008. Downscaling precipitation to river basin in India for IPCC SRES scenarios using support vector machine. International Journal of Climatology 28 (3), 401–420.

Arnold, J.G., Allen, P.M., 1996. Estimating hydrologic budgets for three Illinois watersheds. Journal of Hydrology 176 (1–4), 57–77.

Arnold, J.G., Allen, P.M., Bernhardt, G., 1993. A comprehensive surface groundwater flow model. Journal of Hydrology 142, 47–69.

Beasley, D.B., Monke, E.J., Huggins, L.F., 1977. ANSWERS: A Model for Watershed Planning. Purdue Agricultural Experimental Station Paper No. 7038. Purdue University, West Lafayette, Indiana.

Buishand, T., Shabalova, M., Brandsma, T., 2004. On the choice of the temporal aggregation level for statistical downscaling of rainfall. Journal of Climate 17, 1816–1827.

Carter, T.R., Parry, M.L., Harasawa, H., Nishioka, S., 1994. IPCC Technical Guidelines for Assessing Climate Change Impacts and Adaptations. University College, London.

Central Water Commission, 2005. Water Data Complete Book – 2005. http:/www.cwc.nic.in/main/downloads/Water_Data_Complete_Book_2005.

Chen, S.T., Yu, P.S., Tang, Y.H., 2010. Statistical downscaling of daily precipitation using support vector machines and multivariate analysis. Journal of Hydrology 385, 13–22.

Chu, J.T., Xia, J., Xu, C.Y., Singh, V.P., 2010. Statistical downscaling of daily mean temperature, pan evaporation and rainfall for climate change scenarios in Haihe River, China. Theoretical and Applied Climatology 99 (1–2), 149–161.

Collins, M., Tett, S.F.B., Cooper, C., 2001. The internal climate variability of HadCM3, a version of the Handley Center coupled model without flux adjustments. Climate Dynamics 17, 61–81.

Courant, R., Hilbert, D., 1970. Methods of Mathematical Physics, vols. I and II. Wiley Interscience, New York.

Deb, P., Shrestha, S., Babel, M.S., 2014. Forecasting climate change impacts and evaluation of adaptation options for maize cropping in the hilly terrain of Himalayas: Sikkim, India. Theoretical and Applied Climatology 1–19. http://dx.doi.org/10.1007/s00704-014-1262-4.

Duhan, D., Pandey, A., 2014. Statistical downscaling of temperature using three techniques in the Tons River basin in Central India. Theoretical and Applied Climatology 1–18. http://dx.doi.org/10.1007/s00704-014-1253-5.

El-Sadek, A., Bleiweiss, M., Shukla, M., Guldan, S., Fernald, A., 2011. Alternative climate data sources for distributed hydrological modeling on a daily time step. Hydrological Processes 25 (10), 1542–1557.

Fowler, H.J., Ekström, M., Kilsby, C.G., Jones, P.D., 2005. New estimates of future changes in extreme rainfall across the UK using regional climate model integrations. 1: assessment of control climate. Journal of Hydrology 300, 212–233.

Ghosh, S., Mujumdar, P.P., 2008. Statistical downscaling of GCM simulations to streamflow using relevance vector machine. Advances in Water Resources 31, 132–146.

Gosain, A.K., Mani, A., Dwivedi, C., 2009. Hydrological Modeling-literature Review. Report No-1, Climawater, a Indo-norwegian Institutional Cooperation Program, 2009–2011.

Guo, S., Wang, J., Xiong, L., Ying, A., Li, D., 2002. A macro-scale and semi-distributed monthly water balance model to predict climate change impacts in China. Journal of Hydrology 268, 1–15.

Hargreaves, G.H., Samani, Z.A., 1982. Estimating potential evapotranspiration. Journal of the Irrigation and Drainage Division 108 (3), 225–230.

Hargreaves, G.H., Samani, Z.A., 1985. Reference crop evapotranspiration from temperature. Applied Engineering in Agriculture 1 (2), 96–99. http://dx.doi.org/10.13031/2013.26773.

Hassan, Z., Shamsudin, S., Harun, S., 2013. Application of SDSM and LARS-WG for simulating and downscaling of rainfall and temperature. Theoretical and Applied Climatology. http://dx.doi.org/10.1007/s00704-013-0951-8.

Houghton, J.T., Ding, Y.D.J.G., Griggs, D.J., Noguer, M., van der Linden, P.J., Dai, X., Maskell, K., Johnson, C.A., 2001. Climate Change 2001: The Scientific Basis. Cambridge University Press, Cambridge, p. 881.

Hulme, M., Jenkins, G.J., Lu, X., Turnpenny, J.R., Mitchell, T.D., Jones, R.G., Lowe, J., Murph, J.M., Hassell, D., Boorman, P., McDonald, R., Hill, S., 2002. Climate Change Scenarios for the United Kingdom: the UKCIP02 Scientific Report, Tyndall Centre for Climate Change Research. School of Environmental Sciences, University of East Anglia, Norwich, UK, p. 120.

Hush, D.R., Horne, B.G., 1993. Progress in supervised neural networks-what's new since Lippmann. IEEE Signal Processing 8–39.

IPCC (Intergovernmental Panel on Climate Change), 2007. Climate Change: Impacts, Adaptation and Vulnerability. Contribution of Working Group II to the Fourth Assessment Report of IPCC. Cambridge, United Kingdom and New York, USA, p. 976.

Ito, A., 2007. Simulated impacts of climate and land-cover change on soil erosion and implication for the carbon cycle, 1901–2100. Geophysical Research Letters 34 (9), L09403. http://dx.doi.org/10.1029/2007GL029342.

Kalnay, E., Kanamitsu, M., Kistler, R., Collins, W., Deaven, D., Gandin, L., Iredell, M., Saha, S., White, G., Woolen, J., Zhu, Y., Chelliah, M., Ebisuzaki, W., Higgins, W., Janowiak, J., Mo, K.C., Ropelewski, C., Wang, J., Leetma, A., Reynolds, R., Jenne, R., Joseph, D., 1996. The NCEP/NCAR 40-year reanalysis project. Bulletin of the American Meteorological Society 77, 437–471.

Kamga, F.M., 2001. Impact of greenhouse gas induced climate change on the runoff of the Upper Benue River (Camernoon). Journal of Hydrology 252, 145–156.

Kannan, S., Ghosh, S., 2011. Prediction of daily rainfall state in a river basin using statistical downscaling from GCM output. Stochastic Environmental Research and Risk Assessment 25 (4), 457–474.

Keerthi, S.S., Lin, C.J., 2003. Asymptotic behaviors of support vector machines with Gaussian kernel. Neural Computation 15 (7), 1667–1689.

Khalili, M., Brissette, F., Leconte, R., 2009. Stochastic multi-site generation of daily weather data. Stochastic Environmental Research and Risk Assessment 23, 837–849. http://dx.doi.org/10.1007/s00477-008-0275-x.

Kidson, J.W., Renwick, J.A., 2002. Patterns of convection in the tropical Pacific and their influence on New Zealand weather. International Journal of Climatology 22, 151–174.

Kothawale, D.R., Kumar, K.K., Srinivasan, G., 2012. Spatial asymmetry of temperature trends over India and possible role of aerosols. Theoretical and Applied Climatology 110 (1–2), 263–280.

Kundu, S., Mondal, A., Khare, D., Mishra, P.K., Shukla, R., 2014. Shifting shoreline of Sagar Island Delta, India. Journal of Maps 10 (4), 612–619.

Laflen, J.M., Elliot, W.J., Simanton, J.R., Holzhey, S., Kohl, K.D., 1991. WEPP soil erodibility experiments for rangeland and cropland soils. Journal of Soil Water Conservation 46 (1), 39–44.

Leander, R., Buishand, T.A., 2007. Resampling of regional climate model output for the simulation of extreme river flows. Journal of Hydrology 332 (3), 487–496.

Loo, Y.Y., Billa, L., Singh, A., 2015. Effect of climate change on seasonal monsoon in Asia and its impact on the variability of monsoon rainfall in Southeast Asia. Geoscience Frontiers 6 (6), 817–823.

Meenu, R., Rehana, S., Mujumdar, P.P., 2013. Assessment of hydrologic impacts of climate change in Tunga–Bhadra river basin, India with HEC-HMS and SDSM. Hydrological Processes 27 (11), 1572–1589.

Mercer, J., 1909. Functions of positive and negative type and their connection with the theory of integral equations. Philosophical Transactions of the Royal Society of London 209 (A-456), 415–446.

Mondal, A., Khare, D., Kundu, S., Meena, P.K., Mishra, P.K., Shukla, R., 2014. Impact of climate change on future soil erosion in different slope, land use, and soil-type conditions in a part of the Narmada river basin, India. Journal of Hydrologic Engineering. http://dx.doi.org/10.1061/(ASCE)HE.1943-5584.0001065.

Nash, J., Sutcliffe, J.V., 1970. River flow forecasting through conceptual models part I—A discussion of principles. Journal of Hydrology 10 (3), 282–290.

Rai, A., Joshi, M.K., Pandey, A.C., 2012. Variations in diurnal temperature range over India: under global warming scenario. Journal of Geophysical Research 117, D02114.

Raje, D., Mujumdar, P.P., 2011. A comparison of three methods for downscaling daily rainfall in the Punjab region. Hydrological Processes 25, 3575–3589.

Raneesh, K.Y., Thampi, S.G., 2013. Bias correction for RCM predictions of precipitation and temperature in the Chaliyar river basin. Journal of Climatology & Weather Forecasting 1 (2), 1–6.

Rehana, S., Mujumdar, P.P., 2013. Regional impacts of climate change on irrigation water demands. Hydrological Processes 27 (20), 2918–2933.

Rouhani, H., Willems, P., Wyseure, G., Feyen, J., 2007. Parameter estimation in semi-distributed hydrological catchment modelling using a multicriteria objective function. Hydrological Processes 21, 2998–3008.

Rupa Kumar, K., Sahai, A.K., Kumar, K.K., Patwardhan, S.K., Mishra, P.K., Revadekar, J.V., Kamala, K., Pant, G.B., 2006. High-resolution climate change scenarios for India for the 21st century. Current Science 90 (3), 334–345.

Schnur, R., Lettenmaier, D.P., 1998. A case study of statistical downscaling in Australia using weather classification by recursive partitioning. Journal of Hydrology 212/213, 362–379.

Shi, P., Hou, Y., Xie, Y., Chen, C., Chen, X., Li, Q., Qu, S., Fang, X., Srinivasan, R., 2013. Application of a SWAT model for hydrological modeling in the Xixian

Watershed, China. Journal of Hydrologic Engineering 18, 1522–1529. http://dx.doi.org/10.1061/(ASCE)HE.1943-5584.0000578.
Suykens, J.A., 2001. Nonlinear modelling and support vector machines. In: Instrumentation and Measurement Technology Conference, Budapest, Hungary, 2001. IMTC 2001. Proceedings of the 18th IEEE, vol. 1. IEEE, pp. 287–294.
Suykens, J.A., Vandewalle, J., 1999. Least squares support vector machine classifiers. Neural Processing Letters 9 (3), 293–300.
Thampi, S.G., Raneesh, K.Y., Surya, T.V., 2010. Influence of scale on SWAT model calibration for streamflow in a river basin in the humid tropics. Water Resources Management 24, 4567–4578.
Toews, M.W., Allen, D.M., 2009. Evaluating different GCMs for predicting spatial recharge in an irrigated arid region. Journal of Hydrology 374 (3–4), 265–281. http://dx.doi.org/10.1016/j.jhydrol.2009.06.022.
Tripathi, S., Srinivas, V.V., Nanjundiah, R.S., 2006. Downscaling of precipitation for climate change scenarios: a Support Vector Machine approach. Journal of Hydrology 330 (3), 621–640.
Vicente-Serrano, S.M., Azorin-Molina, C., Sanchez-Lorenzo, A., Revuelto, J., López-Moreno, J.I., González-Hidalgo, J.C., Moran-Tejeda, E., Espejo, F., 2014. Reference evapotranspiration variability and trends in Spain, 1961–2011. Global and Planetary Change 121, 26–40.
Wetterhall, F., Halldin, S., Xu, C., 2005. Statistical rainfall downscaling in central Sweden with the analogue method. Journal of Hydrology 306, 174–190.
Wigley, T.M.L., Jones, P.D., Briffa, K.R., Smith, G., 1990. Obtaining subgrid- scale information from coarse-resolution general circulation model output. Journal of Geophysical Research 95 (D2), 1943–1953.
Wilks, D.S., 1998. Multisite generalization of a daily stochastic rainfall generation model. Journal of Hydrology 210, 178–291.
Yang, D., Kanae, S., Oki, T., Koike, T., Musiake, K., 2003. Global potential soil erosion with reference to land use and climate changes. Hydrological Processes 17, 2913–2928.
Young, R.A., Onstad, C.A., Bosch, D.D., Anderson, W.P., 1989. AGNPS: a nonpoint source pollution model for evaluating agricultural watershed. Journal of Soil and Water Conservation 44, 168–173.
Young, R.A., Onstad, C.A., Bosch, D.D., Anderson, W.P., 1987. AGNPS: An Agricultural Nonpoint Source Pollution Model: A Large Watershed Analysis Tool. Conservation Research Rep. 35. U.S. Department of Agriculture, Washington, DC.
Zhang, G.H., Nearing, M.A., Liu, B.Y., 2005. Potential effects of climate change on rainfall erosivity in the Yellow River basin in China. Transactions of the ASAE 48, 511–517.

Please cite this article in press as: Kundu, S., et al., Future changes in rainfall, temperature and reference evapotranspiration in the central India by Least Square Support Vector Machine, Geoscience Frontiers (2016), http://dx.doi.org/10.1016/j.gsf.2016.06.002